

# Circular Dichroism Spectroscopy Using Coherent Laser-Induced Thermal Gratings

David W. Neyer, Larry A. Rahn, David W. Chandler,\* Jon A. Nunes,<sup>†</sup> and William G. Tong

Contribution from the Combustion Research Facility, Sandia National Laboratories, Livermore, California 94551, and Department of Chemistry, San Diego State University, San Diego, California 92182

Received January 28, 1997. Revised Manuscript Received June 4, 1997<sup>⊗</sup>

**Abstract:** A new pulsed four-wave mixing technique for the detection and real-time measurement of circular dichroism (CD) in liquid samples is demonstrated. The technique is based on the formation and detection of transient thermal gratings formed by the interference of two laser beams whose polarizations are controlled and modulated using a photoelastic modulator. Through an internal heterodyne process, coherent thermal gratings interfere to greatly enhance a weak circular dichroism signal. By measuring the ratio of the difference of scattered laser light from two different polarizations,  $\Delta S$ , to the average amount of scattered light,  $S_{\text{ave}}$ , one can determine the value of  $\Delta\epsilon/\epsilon$  for the compound under investigation. Samples of chiral camphorquinone are used to demonstrate the technique in the ultraviolet region of the spectrum. These studies of camphorquinone, which has a value of  $\Delta\epsilon/\epsilon \approx 10^{-3}$  at 266 nm, produce values of  $\Delta S/S_{\text{ave}}$  which are orders of magnitude larger than  $\Delta\epsilon/\epsilon$  and which approach 2 (the mathematical limit for  $\Delta S/S_{\text{ave}}$ ). Possible extensions of the technique for measuring CD in very small sample volumes and monitoring time-dependence are discussed.

## Introduction

Chirality in molecular systems has been widely studied due to the fundamental role optically active species play in nature.<sup>1</sup> Investigations of the structural and biological properties associated with chirality are of great interest in both fundamental and applied areas of science. Many biological organic compounds, as well as numerous inorganic complexes, exhibit optical activity and are the subjects of intense research in chemical, biological, and biomedical laboratories. For example, the pharmacological effects of stereoisomers<sup>2,3</sup> can be dramatically different and must be understood and monitored to avoid potential health risks.<sup>4</sup> Sensitive detection of chirality is therefore a particularly important, although challenging, experimental goal. By employing a novel heterodyne technique with laser-induced thermal gratings, we have been able to demonstrate enhanced detection of chirality using circular dichroism.

Circular dichroism (CD) is a powerful tool for measuring optical activity. The ability to assign structural features of molecular systems to specific regions of a CD spectrum often makes CD preferential to other measurements of chirality, such as optical rotation.<sup>5–7</sup> Circular dichroism is typically characterized either by the difference in absorption between left- and right-handed circularly polarized light ( $\Delta\epsilon = \epsilon_L - \epsilon_R$ ) or by the ratio of this difference to the average absorption ( $\Delta\epsilon/\epsilon$ ). In many systems of interest, the value of  $\Delta\epsilon/\epsilon$ , often called the

dissymmetry ratio, is between  $10^{-2}$  and  $10^{-4}$ . To measure chirality, conventional CD spectroscopy techniques rely on the ability to detect small changes between absorption signals for two polarizations and consequently require very stable light sources and long signal-averaging times. Due to the inherently small magnitude of CD signals, these conventional techniques have long been plagued with detection sensitivity problems.<sup>8</sup>

Laser-induced grating spectroscopy (LIGS), four-wave mixing (FWM) spectroscopy, has proven to be a powerful tool for probing the chemical and physical properties of numerous chemical samples in many different environments.<sup>9–11</sup> In absorbing liquids, thermally induced nonlinear effects often dominate other types of nonlinearities in the generation of the signal, and FWM has been demonstrated to be an excellent technique for measuring weak absorbances in liquid analytes.<sup>12–14</sup> Unlike conventional absorption techniques which are “transmissive” in nature (*i.e.*, the desired measurement is derived from a small difference in two large signals), FWM is a “dark background” technique. The measured signal is a coherent laser beam that emerges at a specific angle from the sample, away from the input laser beams, and against a virtually dark background (*i.e.*, the signal beam is generated only when the analyte absorbs).

Since FWM is well suited for measuring small absorbances in liquids, it is a good candidate for the measurement of circular dichroism. While second harmonic generation has been

<sup>†</sup> Permanent address: Corning Nichols Institute, 33608 Ortega Highway, San Juan Capistrano, CA 92690.

<sup>⊗</sup> Abstract published in *Advance ACS Abstracts*, August 1, 1997.

(1) Mason, S. F. *Optical Activity and Chiral Discrimination*; D. Reidel Publishing Co.: Dordrecht, Holland, 1979; Vol. 48.

(2) Stinson, S. C. *Chem. Eng. News* **1993**, *71*, 38.

(3) Stinson, S. C. *Chem. Eng. News* **1994**, *72*, 38.

(4) Blaschke, G.; Kraft, H. P.; Fickentscher, K. F. *Arzneim.-Forsch.* **1979**, *29*, 1640–1642.

(5) Purdie, N.; Swallows, K. A. *Anal. Chem.* **1989**, *61*, 77A–89A.

(6) Grosjean, M.; Legrand, M.; Velluz, L. *Optical Circular Dichroism*; Academic Press, Inc.: New York and London, 1965.

(7) Purdie, N.; Brittain, H. G. *Analytical Applications of Circular Dichroism*; Elsevier: Amsterdam and New York, 1994; Vol. 14.

(8) Geng, L.; McGown, L. B. *Anal. Chem.* **1994**, *66*, 3243–3246.

(9) Eichler, H. J.; Gunter, P.; Pohl, D. W. *Laser-Induced Dynamic Gratings*; Springer-Verlag: Berlin, 1986; Vol. 50 and references therein.

(10) Hall, G.; Whitaker, B. J. *J. Chem. Soc., Faraday Trans.* **1994**, *90*, 1–16 and references therein.

(11) Zhu, X. R.; McGraw, D. J.; Harris, J. M. *Anal. Chem.* **1992**, *64*, 710–719.

(12) Harris, J. M.; Pelletier, M. J.; Thorshelm, H. R. *Anal. Chem.* **1982**, *54*, 239–242.

(13) Wu, Z.; Tong, W. G. *Anal. Chem.* **1989**, *61*, 998–1001.

(14) Wu, Z.; Tong, W. G. *Anal. Chem.* **1991**, *63*, 1943–1947.

used successfully to measure CD at surfaces and interfaces<sup>15–20</sup> and higher-order nonlinearities have been observed in concentrated chiral solutions,<sup>21–23</sup> Nunes and Tong<sup>24</sup> were the first to demonstrate sensitive CD measurements in an isotropic liquid sample using a nonlinear laser spectroscopic technique. CD measurements were conducted using a degenerate four-wave mixing (DFWM) geometry, a continuous wave laser for grating formation and detection, and a Pockel cell for polarization modulation (modulation of one of the grating forming beams between left- and right-circular polarization). The nonlinear DFWM-CD design is similar to more conventional CD measurement techniques that use polarization modulation and signal subtraction to determine  $\Delta\epsilon$ . However DFWM-CD offers many advantages, including a coherent CD signal beam, excellent spatial resolution, and high signal-to-noise ratio.

Further work by Nunes *et al.*<sup>25</sup> and by Terazima<sup>26,27</sup> showed that CD could be detected using only a polarization grating. When cross-polarized pump beams are employed, a polarization grating is generated in the sample. In chiral samples, differential absorption across the grating fringes results in a thermal grating that can scatter an impinging probe beam to generate the signal. A fundamental difference between this technique and the initial work of Nunes and Tong<sup>24</sup> is that the CD signal is on a true zero background and does not depend on subtraction modulation techniques to derive the signal. However, the signals in these experiments are often very weak. In the studies of Nunes *et al.*, a continuous wave laser was used which eliminated problems with shot-to-shot power fluctuations common in pulsed lasers. While Terazima's experiments employed pulsed dye lasers, the measurements were made using the more sensitive phase-matched (or "thick grating") detection technique, which is less easily tunable for collection of CD spectra. The work of Nunes *et al.* also showed that coherent intensity and polarization gratings in the sample can interfere when the laser polarizations are slightly modified.

In this paper we demonstrate a new pulsed laser technique for measuring CD that exploits the interference between intensity and polarization gratings in the sample and overcomes many of the problems associated with both conventional and previous nonlinear CD measurements. As with the previous laser-induced grating schemes, the technique is based on the formation and detection of transient thermal gratings formed by the interference of two laser beams. Through modulation of the laser polarizations, an interference between two types of thermal gratings is produced which can be sensitively monitored. The method is similar to the heterodyne techniques used in coherent Raman and frequency-modulation spectroscopies and is motivated by the same need to optimize the signal-to-noise ratio.<sup>28</sup>

(15) Yee, H. I.; Byers, J. D.; Petralli-Mallow, T.; Hicks, J. M. *SPIE Conf. Proc.* **1993**, *1858*, 343–353.

(16) Petralli-Mallow, T.; Wong, T. M.; Byers, J. D.; Yee, H. I.; Hicks, J. M. *J. Phys. Chem.* **1993**, *97*, 1383–1388.

(17) Yee, H. I.; Byers, J. D.; Hicks, J. M. *SPIE Conf. Proc.* **1994**, *2125*.

(18) Byers, J. D.; Yee, H. I.; Petralli-Mallow, T.; Hicks, J. M. *Phys. Rev. B* **1994**, *49*, 14643–14647.

(19) Byers, J. D.; Yee, H. I.; Hicks, J. M. *J. Chem. Phys.* **1994**, *101*, 6233–6241.

(20) Byers, J. D.; Hicks, J. M. *Chem. Phys. Lett.* **1994**, *231*, 216–24.

(21) Rentzepis, P. M.; Giordmaine, J. A.; Wecht, K. W. *Phys. Rev. Lett.* **1966**, *16*, 792.

(22) Dubrovskii, A. V.; Koroteev, N. I.; Shkurinov, A. P. *JETP Lett.* **1993**, *56*, 551–557.

(23) Shkurinov, A. P.; Dubrovskii, A. V.; Koroteev, N. I. *Phys. Rev. Lett.* **1993**, *70*, 1085–1088.

(24) Nunes, J. A.; Tong, W. G. *Anal. Chem.* **1993**, *65*, 2990–2994.

(25) Nunes, J. A.; Tong, W. G.; Chandler, D. W.; Rahn, L. A. *J. Phys. Chem.* **1997**, *101*, 3279.

(26) Terazima, M. *J. Phys. Chem.* **1995**, *99*, 1834–1836.

(27) Terazima, M. *Mol. Phys.* **1996**, *88*, 1223–1236.

(28) Levenson, M. D.; Kano, S. S. *Introduction to Nonlinear Laser Spectroscopy*; Revised ed.; Academic Press, Inc.: Boston, MA, 1988.

When the ratio of the difference of scattered laser light from two different polarizations,  $\Delta S$ , to the average amount of scattered light,  $S_{\text{ave}}$ , is measured, one can determine the value of  $\Delta\epsilon/\epsilon$  for the compound under investigation. When complete destructive interference between the thermal gratings causes the signal from one polarization to go to 0, the ratio  $\Delta S/S_{\text{ave}}$  reaches its theoretical limit of 2. This complete interference can be obtained by controlling the ellipticity of the polarized laser light. Samples of chiral camphorquinone in ethanol are used to demonstrate the technique. Experiments on camphorquinone, which has a value of  $\Delta\epsilon/\epsilon \approx 10^{-3}$  at the 266 nm excitation wavelength employed in this study, produce values of  $\Delta S/S_{\text{ave}}$  which approach this limiting value of 2 when maximized. In contrast, a conventional absorption CD measurement on this system would give signals with  $\Delta S/S_{\text{ave}} = \Delta\epsilon/\epsilon \approx 10^{-3}$ . The frequency-quadrupled (266 nm) output of a pulsed Nd:YAG laser is used to make the measurements. The large values of  $\Delta S/S_{\text{ave}}$  in these experiments, along with the demonstrated ability to measure small values of  $\Delta\epsilon/\epsilon$  with an ultraviolet, pulsed laser, indicate that this technique provides a potentially powerful method for measuring static and time-dependent circular dichroism spectra.

## Theory

The theory of laser-induced gratings<sup>9</sup> has been used to describe many four-wave mixing processes, and is particularly useful for understanding the thermal grating<sup>29,30</sup> effects present in these experiments. In a typical LIGS experiment, two laser beams of the same wavelength are crossed at a small angle in the sample. The two beams interfere in the interaction region creating a spatial modulation in the resultant electric field. The response of the sample to this modulated electric field leads to the creation of a grating-type structure which can be probed by the scattering of a third laser beam. The probe beam, which can be the same wavelength as the grating beams (*i.e.*, degenerate four-wave mixing) or a different color, is scattered by the grating to produce a fourth light beam which has the same wavelength and very similar coherence and collimation to the probe beam. In some experimental geometries, the scattered beam is in fact phase-conjugate to the incoming probe beam. Many different physical responses in a sample, with a wide variety of time scales, can be probed using gratings.

In our experiments, the spatial modulation in the electric field due to the interference of our grating laser beams leads to a spatial modulation in the absorption of the solute in our sample. Radiationless relaxation of the excited molecules produces a spatial modulation in the local temperature and a corresponding modulation in the refractive index,  $n$ , of the solution. This response is referred to as thermal grating formation. It is the spatially modulated refractive index which acts as a phase grating and scatters the impinging probe beam. The intensity of the scattered probe beam, or the diffraction efficiency of the grating, is proportional to the square of the modulation depth of the index of refraction,  $(\Delta n)^2$ .

The formation of thermal gratings depends directly on the polarizations of the two "pump" beams which interfere. When the two beams are linearly polarized with parallel polarizations, the interference fringes correspond to a spatial modulation in the intensity (an "intensity grating") of the electric field with valleys where the two fields are out-of-phase and peaks where they are in phase. Pump beams with the same linear polarizations (see Figure 1) create a sinusoidally modulated intensity

(29) Buntine, M. A.; Chandler, D. W.; Hayden, C. C. *J. Chem. Phys.* **1995**, *102*, 2718–2726.

(30) Smith, A. P.; Hall, G.; Whitaker, B. J.; Astill, A. G.; Neyer, D. W.; Delve, P. A. *Appl. Phys. B* **1995**, *60*, 11–18.

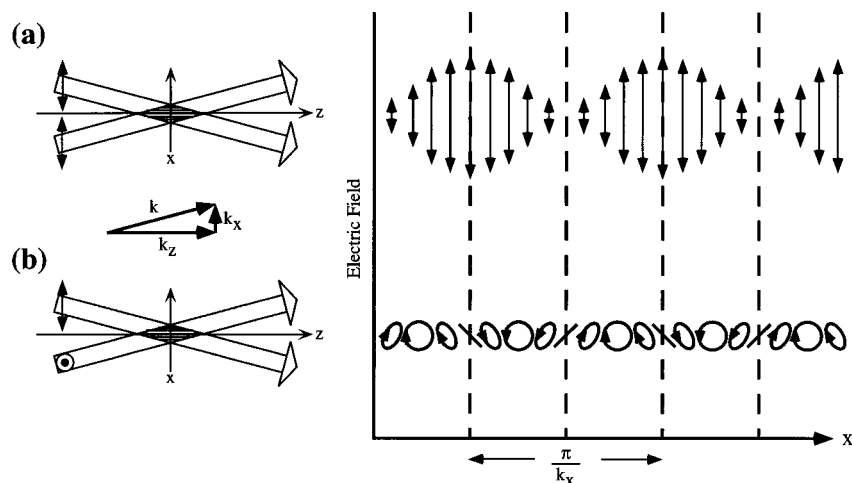


**Figure 1.** (a) Polarization scheme for creation of an intensity grating with corresponding resultant electric field pattern within interaction zone. (b) Polarization scheme for creation of a polarization grating with corresponding electric field picture.

pattern in the crossover region of the two beams. The pattern resembles a conventional diffraction grating composed of light and dark interference fringes. Absorption and subsequent radiationless relaxation by the sample across the interaction zone is modulated, with greater absorption at the intensity maxima and lower at the intensity minima. The magnitude of the resulting thermal grating ( $\Delta n$ ) is proportional to the absorption strength of the sample ( $\epsilon$ ). When the pump beams have perpendicular linear polarizations, the interference yields a spatial modulation in the polarization, but not the intensity, of the resulting electric field (a "polarization grating").<sup>31</sup> As shown in Figure 1, the polarization grating is characterized by modulation between right- and left-handed circular polarization with regions of elliptical and linear polarization in between. In a randomly oriented, nonchiral sample there is equal absorption (which is only proportional to the light intensity) throughout the region, and no thermal grating is formed. However, a chiral sample preferentially absorbs circularly polarized light of one handedness more than the other. Therefore, a polarization grating in a chiral sample leads to differential absorption and the formation of a thermal grating with an amplitude that is proportional to this difference ( $\Delta\epsilon$ ).

When the polarizations of the two pump beams are neither linear parallel nor linear perpendicular, the interference grating is characterized by a complex pattern of both intensity and polarization variations. One can decompose this complex grating into contributions from intensity gratings and polarization gratings with specific spatial phase relationships. Each of these components contributes to the spatial modulation in the index of refraction. While the spatial phases of these individual gratings depend on the relative temporal phase shifts of the different polarization components of the pump beams, the magnitudes depend on the amplitudes of these components. Therefore, the individual gratings have different magnitudes and are shifted spatially. The total thermal grating is then a coherent sum of these components, and the diffracted probe beam intensity is proportional to the square of the magnitude of the total grating. When the polarizations of the two interfering pump beams are carefully controlled, one can control both the magnitudes and the phases of the intensity grating contributions (proportional to  $\epsilon$ ) and the polarization grating contributions (proportional to  $\Delta\epsilon$ ) to the overall thermal grating and produce a total signal which is due to the interference between the two. This method is essentially a heterodyne experiment in which the interference is between two types of thermal grating signals

from the sample rather than between a sample response and an external reference beam.

When the interfering laser beams can be described as monochromatic plane waves (as will be assumed here), the spatial modulation in the resulting electric field, and therefore the index of refraction, across the grating is sinusoidal with a spatial frequency  $2k_x$  (see Figure 1).<sup>9</sup> Because the intensity and polarization grating components that contribute to the total thermal grating are all formed by the same two pump beams, they all have the same value of  $k_x$  and therefore the same spatial frequency. Therefore, one can simply describe the modulated index of refraction for each thermal grating component,  $\delta n_i$ , by a cosine function along the spatial coordinate,  $x$ , with amplitude,  $\Delta n_i$ , and phase,  $\phi_i$ :

$$\begin{aligned}\delta n_j(x) &= \Delta n_j \cos(2k_x x + \phi_j) \\ &= \text{Re}[\Delta n_j e^{i(2k_x x + \phi_j)}] \\ &= \text{Re}[\Delta n_j e^{i\phi_j} e^{i2k_x x}] \quad (1)\end{aligned}$$

The total modulation in the index of refraction,  $\delta n_{\text{tot}}$ , is then simply the sum of the component thermal gratings:

$$\begin{aligned}\delta n_{\text{tot}}(x) &= \sum_j \text{Re}[\Delta n_j e^{i\phi_j} e^{i2k_x x}] \\ &= \text{Re}[\Delta n_{\text{tot}} e^{i\phi_{\text{tot}}} e^{i2k_x x}] \quad (2)\end{aligned}$$

where

$$\Delta n_{\text{tot}} e^{i\phi_{\text{tot}}} = \sum_j (\Delta n_j e^{i\phi_j}) \quad (3)$$

The modulation depth of the total thermal grating is therefore  $\Delta n_{\text{tot}}$ , and the diffraction efficiency of the probe beam is proportional to  $(\Delta n_{\text{tot}})^2$ .

In general, when a chiral sample is investigated using linearly polarized pump beams, with electric fields  $E_1$  and  $E_2$ , both an intensity grating (IG) and a polarization grating (PG) are formed. As one rotates the polarization of  $E_2$  with respect to  $E_1$ , the relative contributions of the two gratings will change. To be consistent with the experiments, we define the angle of rotation,  $\theta$ , to be 0 when the beams are perpendicular. The thermal modulation of the refractive index resulting from the intensity grating (IG) is defined to have  $\phi_{\text{IG}}$  equal to 0 and a modulation depth given by

(31) Fourkas, J. T.; Trebino, R.; Fayer, M. D. *J. Chem. Phys.* **1992**, *97*, 69–77.

$$\Delta n_{\text{IG}} = cE_1 E_{\parallel} \epsilon \quad (4)$$

where

$$E_{\parallel} = E_2 \sin(\theta) \quad (5)$$

is the component of  $E_2$  that is parallel to  $E_1$ . To a first order,  $c$  is assumed to be a constant accounting for the physical parameters of the sample which control the transfer of the modulated absorption to a thermal modulation and to a modulated index of refraction. In comparison, the index of refraction modulation due to the polarization grating (PG) is described by

$$\Delta n_{\text{PG}} = cE_1 E_{\perp} (\Delta\epsilon) \quad (6)$$

and

$$\phi_{\text{PG}} = \pm\pi/2 \quad (7)$$

where

$$E_{\perp} = E_2 \cos(\theta) \quad (8)$$

is the component of  $E_2$  that is perpendicular to  $E_1$ , and the sign of  $\phi_{\text{PG}}$  depends on the sign of  $\Delta\epsilon$ . Since the intensity grating and the polarization grating are spatially  $\pi/2$  out-of-phase, they do not interfere with each other and the overall diffraction efficiency (or signal,  $S$ ) is proportional to the sum of the squares of the two gratings:

$$S \propto \left| \Delta n_{\text{IG}} + \Delta n_{\text{PG}} e^{i(\pi/2)} \right|^2 = (\Delta n_{\text{IG}})^2 + (\Delta n_{\text{PG}})^2 \quad (9)$$

Since  $\Delta\epsilon/\epsilon$  is typically between  $10^{-2}$  and  $10^{-4}$ , the polarization grating signal due to the circular dichroism is often quite weak and the total signal is dominated by the intensity grating even for small nonzero values of  $\theta$ . However, if the relative spatial phase of these two gratings is modulated by  $\pm\psi$ , the gratings will interfere. The scattered signal measured for the shifted gratings is given by

$$S_{\pm} \propto \left| \Delta n_{\text{IG}} + \Delta n_{\text{PG}} e^{i((\pi/2) \pm \psi)} \right|^2 \quad (10)$$

For selected values of  $\psi = (2n + 1)\pi/2$ , the interference will be alternately constructive and destructive. When this interference is exploited to produce a heterodyne signal between the two gratings, one can greatly enhance the sensitivity to the CD-induced polarization grating and measure the small values of  $\Delta\epsilon/\epsilon$  that are typically encountered.

Experimentally, this can be achieved by placing a photoelastic modulator (PEM) in the rotated pump beam ( $E_2$ ) with its optical axis parallel to the polarization of  $E_1$ . The retardation of the PEM is set for quarter wave at the pump wavelength, and the pulsed laser is synchronized with the oscillations of the PEM crystal so that sequential laser pulses emerge with  $E_{\parallel}$  alternately retarded and advanced in time with respect to  $E_{\perp}$ . The quarter wave temporal retardation of the laser polarization components leads to a  $\psi = \pm\pi/2$  shift in the relative spatial phase between the intensity and polarization gratings. When the intensity of the light diffracted from the gratings formed by the sequential laser pulses ( $S_+$  and  $S_-$ ) is measured and the difference between these two signals is calculated

$$\begin{aligned} \Delta S &= S_- - S_+ \\ &= 4\Delta n_{\text{IG}} \Delta n_{\text{PG}} \end{aligned} \quad (11)$$

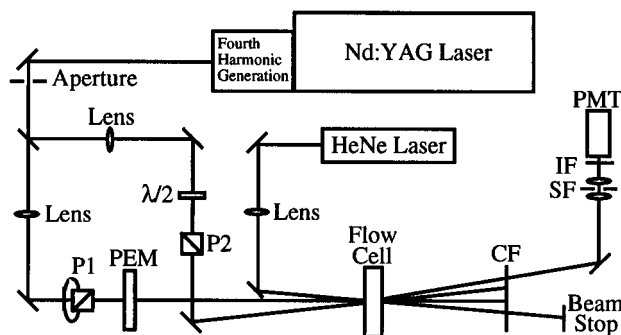


**Figure 2.** Experimental optical setup (P1, polarizer in vertically polarized beam; P2, polarizer in horizontally polarized beam; IF, interference filter; SF, spatial filter; CF, color filter to block 266 nm).

the average of the two

$$\begin{aligned} S_{\text{ave}} &= \frac{S_- + S_+}{2} \\ &= \Delta n_{\text{IG}}^2 + \Delta n_{\text{PG}}^2 \end{aligned} \quad (12)$$

and the ratio between them

$$\begin{aligned} \frac{\Delta S}{S_{\text{ave}}} &= \frac{4\Delta n_{\text{IG}} \Delta n_{\text{PG}}}{\Delta n_{\text{IG}}^2 + \Delta n_{\text{PG}}^2} \\ &= \frac{4(\Delta\epsilon/\epsilon) \cos(\theta) \sin(\theta)}{(\Delta\epsilon/\epsilon)^2 \cos^2(\theta) + \sin^2(\theta)} \end{aligned} \quad (13)$$

one can make high contrast measurements of the dissymmetry ratio,  $\Delta\epsilon/\epsilon$ , for the sample. The  $\pm$  signs depend on both the sign of  $\Delta\epsilon/\epsilon$  and the phase of the PEM crystal oscillation. While in these experiments the sign of  $\Delta\epsilon/\epsilon$  was known from the chemical samples, in general it can be determined directly from the experimental parameters.

The presented experimental scheme, in which the angle of the linearly polarized light entering the PEM is rotated, provides the simplest theoretical treatment and most direct analysis. In this case, the light emerging from the PEM is elliptically polarized with the major axis of the ellipse parallel to the original linear polarization axis. This configuration leads to the formation of only two thermal gratings in the sample (one intensity grating and one polarization grating) which are alternately in-phase and out-of-phase and can lead to complete destructive interference and the largest values of  $\Delta S/S_{\text{ave}}$ . However, there are other possible procedures for varying the ellipticity of the laser light which can provide experimental advantages while still allowing one to control the coherence and interference of thermal gratings in the sample. Some of these schemes (including changing the angle and/or retardation of the PEM) have been demonstrated in the laboratory (see Discussion) and change not only the ratio of the major to minor axes of the polarization ellipse of  $E_2$  but also the angle between these axes and the polarization of  $E_1$ . These situations can be treated theoretically by considering the formation of multiple intensity and polarization gratings with appropriate phases using the formalism presented here (eqs 1–3).

## Experimental Section

The optical setup for the experiment is shown in Figure 2. A 50 Hz injection-seeded pulsed Nd:YAG laser with a pulse width of 5–8 ns (Quanta Ray GCR-4) provides the UV excitation light that forms the laser-induced grating in the sample. The fourth harmonic beam of the Nd:YAG laser (266 nm) is separated and sent into the experimental

setup where it is split (50/50), weakly focused with 750 mm focal length lenses, and then recombined at the 0.5 mm path length liquid flow cell at an angle of about  $1^\circ$ . The total laser power at the cell is about 200  $\mu\text{J}$ . A half-wave plate is placed in one of the input beam paths which results in a  $90^\circ$  rotation of the beam's polarization (*i.e.*, the fixed "horizontal" beam). A calcite polarizer is placed after the half-wave plate to purify the linear polarization entering the sample. The other excitation beam is also passed through a calcite polarizer and then through a photoelastic modulator (Hinds PEM-80) before reaching the sample cell. The probe laser is a 5 mW HeNe laser (Uniphase) operating at 632 nm. When thick sample cells are used, phase-matching conditions require that the probe laser beam be scattered at the Bragg angle.<sup>32</sup> However, when a thin sample cell is used (as in the experiments described here) the phase matching constraints are relaxed considerably and the incidence angle of the probe beam is somewhat arbitrary.<sup>33</sup> The HeNe probe is diffracted by the grating into multiple signal beams, one of which is picked off and passed through a spatial filter, a 632 nm laser line filter, and finally is sent to a photomultiplier tube (PMT) for detection. This signal is monitored and averaged with a digital oscilloscope (LeCroy Model 7200/7242B).

The timing for the experiment is controlled by a digital delay generator which in turn is triggered by the PEM. The 50 Hz repetition rate of the YAG laser is synchronized with the PEM so that sequential light pulses from the laser pass through the PEM while the crystal is at opposite extremes of its oscillation. The PEM has a resonant frequency of about 50 kHz, and the YAG laser repetition rate is 50 Hz. This requires a "counting down" of the PEM frequency in order to generate the desired laser pulse-to-pulse polarization modulation. Hence, the delay generator is triggered with the 2f (100 kHz) frequency output from the PEM. This signal is then appropriately counted down, using an odd number of cycles, to generate a 50 Hz frequency that is used to trigger the YAG laser flash lamps and Q-switch. The optical axis of the PEM is aligned vertically, *i.e.*, parallel to the polarization of the incident beam. When the polarizing prism is slightly rotated before the PEM, and therefore, the incident polarization, the modulation of the PEM produces highly eccentric, elliptically polarized light with sequential laser pulses that have equal eccentricity but opposite handedness. The elliptically polarized light interfering with the second horizontally polarized UV laser pulse produces both polarization and intensity gratings in the sample. To systematically change the polarization ellipticity used to create the thermal grating, the polarization of the laser light incident on the PEM is rotated over a small angular range around the vertical ( $\theta = 0$ ) by rotating the polarizing prism. The retardation of the PEM is set for quarter wave at 266 nm so that the phase of the electric field component parallel to the optical axis is shifted by  $\pi/2$  with respect to the perpendicular component. The sign of the phase shift between the two components alternates with sequential laser pulses. The intensity of the diffracted light detected by the PMT is a measure of the amplitude of the overall thermal grating. The diffracted light intensity of sequential laser pulses is measured as a function of the rotation angle of the polarizing prism. These data are used to determine the relative intensities of the polarization and intensity gratings and, therefore, the value of  $\Delta\epsilon/\epsilon$  for the sample.

Optically active (+)- and (-)-camphorquinone was purchased from Sigma Chemicals and used directly. Solutions (20 mM) of these enantiomers were prepared in HPLC grade ethanol, filtered (0.2  $\mu\text{m}$ ), and used immediately after preparation.

## Results

Camphorquinone, a common chiral starting material for organic asymmetric synthesis,<sup>34</sup> has CD bands in the visible and UV regions of the spectrum. Figure 3 shows the UV circular dichroism spectra of the two camphorquinone enantiomers with the position of the pump laser wavelength (266 nm) indicated on the spectra. The wavelength of the UV pump laser used in the grating experiments falls where there is strong absorption, but where the circular dichroism is less than half of

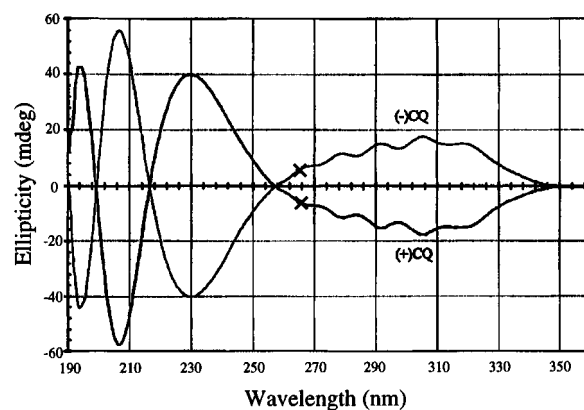


**Figure 3.** Circular dichroism spectra for (+) and (-)-camphorquinone using a conventional CD spectrometer. The 266 nm wavelength used in the laser studies is indicated with an "x".

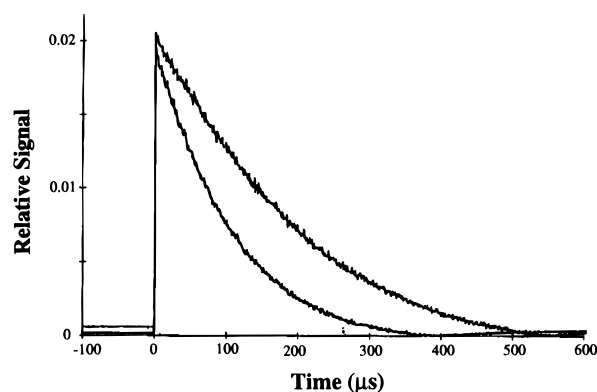


**Figure 4.** Four-wave mixing signal rise and decay for two different crossing angles of the "pump" beams. The faster decay of  $\sim 245 \mu\text{s}$  is for a pump beam crossing angle of  $1.9^\circ$ , while the longer decay of  $\sim 470 \mu\text{s}$  is for  $1.4^\circ$ .

the maximum in the UV. The red HeNe probe laser wavelength lies in a transparent region of the sample and is also outside of the fluorescence and phosphorescence regions of camphorquinone. Scattered red light not associated with the thermal grating signal arises mostly from stray reflections from the sample cell and Rayleigh scattering from particulate and bubbles in the liquid sample that pass through the probe volume. A clean sample cell and a good sample filtration system greatly reduce the stray light level.

An advantage of using a CW probe laser in a pulsed excitation experiment like this is that the time profile of the laser-induced thermal grating can be observed directly. Figure 4 is a digitized plot of the scattered light signal vs time (colinearly polarized pump beams, no modulation). The signal has a fast rise time indicating that the thermal grating forms very quickly, while the signal decay is much slower. This slow decay is due to the long residence time of the thermal grating that eventually degrades because of molecular diffusion processes and flow of the grating out of the detection region. The decay lifetime is inversely proportional to the square of the crossing angle of the pump laser beams.<sup>35</sup> This long grating lifetime allows filtering of contributions from other fast physical processes such as molecular alignment effects and from optical noise sources such as fluorescence that could adversely effect the CD measurements.

The oscilloscope traces presented in Figure 5 illustrate the large variations in signal intensities that are observed with a chiral sample in these heterodyne experiments. The averaged traces for three samples of camphorquinone in ethanol (20 mM)

(32) Siegman, A. E. *J. Opt. Soc. Am.* **1977**, *67*, 545–550.

(33) Moharam, M. G.; Gaylord, T. K.; Magnusson, R. *Opt. Commun.* **1980**, *32*, 19–23.

(34) Ellis, M. K.; Golding, B. T.; Watson, W. P. *Chem. Commun.* **1984**, *23*, 1600–1602.

(35) Eichler, H.; Salje, G.; Stahl, H. *J. Appl. Phys.* **1973**, *44*, 5383–5388.

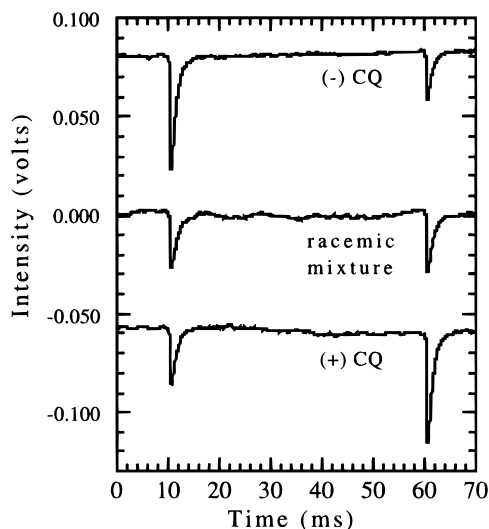


**Figure 5.** Averaged oscilloscope traces showing sequential laser pulses for (+)-camphorquinone, a racemic mixture of the (+)- and (-)-enantiomers, and (-)-camphorquinone. The (+) and (-) sample base lines are offset to distinguish the traces.

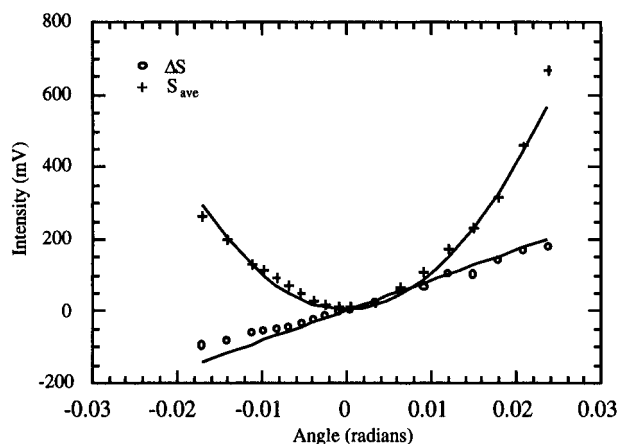


**Figure 6.** Average signal ( $S_{ave}$ ) and difference signal ( $\Delta S$ ) vs polarization rotation for (+)-camphorquinone. The solid lines are calculated using a value of  $\Delta\epsilon/\epsilon = 2 \times 10^{-3}$  (see text).

were taken at a fixed angle of rotation of the polarizing prism where the values of  $\Delta S/S_{ave}$  were near their maxima. The difference in signal intensities for sequential laser pulses in the pure enantiomers is obvious. Also note that the largest scattering signal (constructive interference) occurs on opposite laser pulses for the (+) and (-) samples corresponding to opposite handedness of the elliptically polarized light leaving the PEM. The oscilloscope trace for the racemic mixture of camphorquinone is also presented in Figure 5 and shows no alternation in the signal intensity.

Measurements of the difference in signal,  $\Delta S$ , between the sequential laser pulses and the average signal,  $S_{ave}$ , as the angle of rotation of the polarizing prism is changed are shown in Figure 6 for (+)-camphorquinone. The data are taken directly from the signal peak heights of the averaged oscilloscope traces with no normalization for laser intensity. The two curves shown in Figure 6 are calculated using eqs 11 and 12 with a value of  $\Delta\epsilon/\epsilon = 2 \times 10^{-3}$  and a single intensity normalization factor. While the value of  $\Delta S$  changes nearly linearly for small values of  $\theta$ ,  $S_{ave}$  grows much faster. Also note that the difference signal changes sign as the polarization is rotated from  $\theta$  to  $-\theta$ . A similar plot for (-)-camphorquinone reveals a nearly identical plot of  $S_{ave}$  and a plot of  $\Delta S$  that is the same except for a change in sign (not shown).

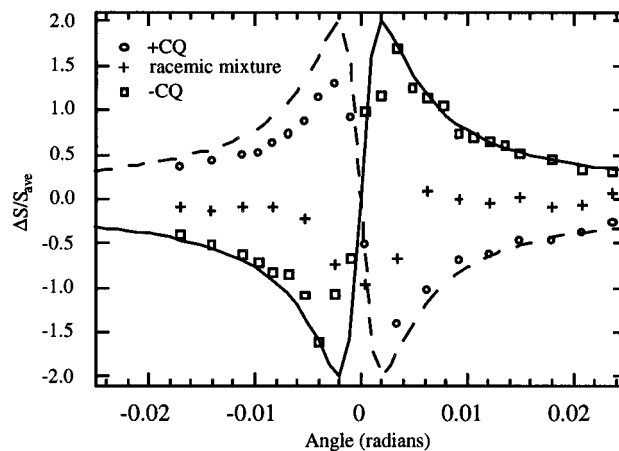


**Figure 7.**  $\Delta S/S_{ave}$  vs rotation for both enantiomers of camphorquinone and a racemic mixture. A constant value of scattered light signal (measured with an ethanol blank) has been subtracted from the raw data. The solid and dashed lines are calculated for the enantiomers using a value of  $\Delta\epsilon/\epsilon = 2 \times 10^{-3}$  (see text).

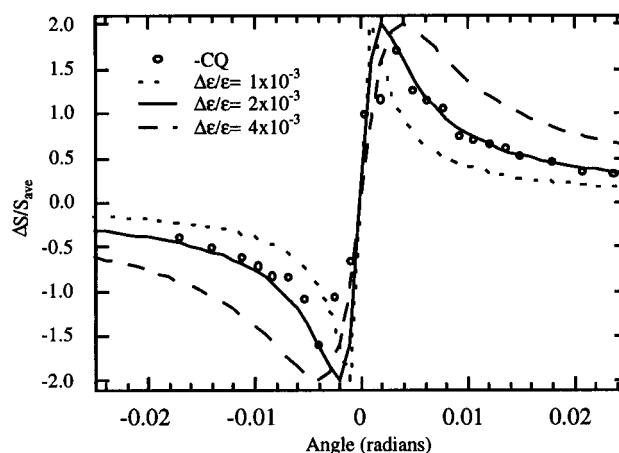


**Figure 8.**  $\Delta S/S_{ave}$  vs rotation for (+)-camphorquinone with a constant amount of scattered light background subtracted. The lines are calculated using eq 13 with  $\Delta\epsilon/\epsilon = 1 \times 10^{-3}$  (···),  $2 \times 10^{-3}$  (—), and  $4 \times 10^{-3}$  (- - -). The improved accuracy of the  $2 \times 10^{-3}$  fit is apparent at the higher angles where the signal-to-noise ratio is optimized between scattered light and technical noise.

Plots of the ratio  $\Delta S/S_{ave}$  for the three samples of camphorquinone are shown in Figure 7 along with calculated curves (eq 13) using  $\Delta\epsilon/\epsilon = 2 \times 10^{-3}$ . A constant scattered light background (measured with a pure ethanol sample) was subtracted from the measured signal intensities. For this experimental configuration which produces only one polarization grating and one intensity grating, the  $\Delta S/S_{ave}$  curve reaches a maximum when the magnitude of the polarization grating equals that of the intensity grating. In the limit of a small angle of rotation ( $\sin \theta \approx \theta$ ), this maximum occurs when  $\theta$ , measured in radians, is equal to  $\Delta\epsilon/\epsilon$ . While such a direct measurement is convenient and provides a reasonably accurate measurement of  $\Delta\epsilon/\epsilon$ , the peak of such a curve occurs when the intensity grating is equal to the typically weak polarization grating. Therefore, the measured signal is quite small and more susceptible to problems such as scattered light. Fitting the data to a calculated curve provides a better method for determining the value of  $\Delta\epsilon/\epsilon$  and can also be applied to experimental procedures in which the signal results from the interference of more than two thermal gratings. Figure 8 shows the (+)-camphorquinone sample data plotted along with theoretical fits using three different values of  $\Delta\epsilon/\epsilon$ . The curve calculated with  $\Delta\epsilon/\epsilon = 2 \times 10^{-3}$  fits quite well to the experimental data, particularly at the slightly larger angles where the signal-to-

noise ratio is optimized between scattered light and technical noise. This value for  $\Delta\epsilon/\epsilon$  is in accord with literature values<sup>36–38</sup> for camphorquinone in ethanol and with that measured by conventional techniques to be  $\sim 5 \times 10^{-3}$ . The figure also demonstrates the large changes that can be seen in the CD signal with relatively small variations in the value of  $\Delta\epsilon/\epsilon$ .

## Discussion

The results presented above show that transient thermal gratings can be used to make sensitive measurements of circular dichroism in small samples with pulsed lasers. Through careful modulation of the polarization of the pump beams, we have been able to produce a heterodyne signal between a relatively weak CD-induced polarization grating and a stronger intensity grating which provides significant enhancement of the CD signal. This enhancement has allowed us to make pulsed measurements of the relatively weak circular dichroism of camphorquinone in the ultraviolet (266 nm) region of the spectrum.

The pulsed nature of this technique also provides great potential for making time-resolved circular dichroism (TRCD) measurements. TRCD can provide a unique method for measuring structural rearrangement and folding for both smaller chiral species and large macromolecules in different environments. Recent advances in measuring TRCD have provided excitement about the possibilities and power of such measurements.<sup>39–41</sup> More conventional TRCD methods are limited by the time scale of the polarization modulator employed. While others can use shorter-pulse lasers, they often depend on the inherently weak difference between two large absorption signals<sup>42</sup> or are ellipsometric and are subject to significant optical artifacts.<sup>43</sup> While the technique described here has employed a photoelastic modulator to alternate the pump laser polarizations, the PEM does not limit the time-response of the measurement. The time-resolution of these CD measurement is only limited by the pulse length of the grating forming (pump) laser. Although the thermal grating may form in microseconds, and in this case is probed with a continuous HeNe laser, it is the chirality of the sample at the time of absorption (during the pump pulse) that determines the magnitude of the resultant signal.

One could therefore initiate a photochemical reaction with a short-pulse laser which leads to a change in the circular dichroism of the sample. This time-dependent change in the CD could be followed by delaying a second laser pulse which is split to form the two pump beams. The thermal grating signal which monitors the CD of the sample will be determined at the time of the pump beam absorptions, but may be “read” with either a CW laser (as done here) or with another delayed laser pulse. The time duration of the probe laser is independent of the time scale for the photochemical changes. This heterodyne grating technique may also allow one to reduce or measure artifacts which occur in many TRCD experiments. For example, the thermal grating method is only susceptible to imperfect optics before the sample. While artifacts will therefore depend

on imperfect polarizers and rotators in the pump beams and birefringence in the first cuvette window, the polarization of the scattered probe beam is not important (in contrast to ellipsometry measurements). The coherent thermal grating technique may also allow one to differentiate the true CD signal from other artifacts such as the linear dichroism induced by initiating the photochemical process with a linearly polarized laser. One could design the experiment such that the thermal grating due to such linear dichroism is spatially out-of-phase with the CD polarization grating (e.g., using an initiation laser linearly polarized at 45° with respect to the pump polarization; see Figure 1). While this “artifact” signal would still be present, one may be able to adjust the grating laser polarizations appropriately to make coherent thermal grating measurements of both this linear dichroism and the true CD signal. There are many possibilities for further exploration and evaluation, but it appears the high contrast measurements of the heterodyne grating technique coupled with widely available short-pulse lasers should provide a powerful tool for measuring TRCD.

Earlier schemes employing transient thermal gratings to measure CD produce significant problems when applied to the samples described here. The small value of  $\Delta\epsilon/\epsilon$  at the studied wavelength along with the shot-to-shot noise of the pulsed laser system make direct measurements of a polarization grating fairly difficult. As shown in Figure 6, the signal from orthogonally polarized pump beams is very small and often comparable to the scattered light level of the experiment. Direct measurements with pulsed lasers were previously demonstrated by Terazima.<sup>26,27</sup> Those measurements were made using visible light with a phase-matched detection geometry. Measurements in the UV suffer from additional complications. Polarization optics do not operate efficiently in the UV region to purify the excitation beams' polarizations so that small CD signals can be measured. Also, the nonlinear optical schemes typically used to generate UV light increase the shot-to-shot power fluctuations in the excitation laser. When the interference between the intensity and polarization gratings is utilized to produce a greatly enhanced heterodyne signal, one can overcome these additional difficulties to make high contrast measurements of CD. The increased sensitivity also allows one to use the non-phase-matched thin grating geometry. This will provide increased flexibility for scanning the wavelength of the excitation laser to record the CD spectrum and the ability to probe very small sample volumes.

While we did not make a systematic study of detection limits with this technique, the experimental results presented are background limited (see Figure 5) in their detection of small concentrations. Imperfect wavelength and spatial filtering to remove scattered pump light along with absorption by the solvent or impurities are likely causes for this background. Nonlinear optical techniques such as the grating technique presented here typically have a concentration dependence which is quadratic or higher. This limits such techniques in the detection of very small concentrations. However, nonlinear techniques are also very sensitive to laser powers and absorption cross sections, and specific optimizations for a given experimental setup are important. While the experiments presented are approaching the background limit for concentration sensitivity, the use of coherent thermal gratings still allows sensitive determination of a small dissymmetry ratio ( $\Delta\epsilon/\epsilon$ ).

Heterodyne techniques have been used in other laser-based detection methods including coherent Raman and absorption spectroscopy.<sup>28</sup> They have also been used in conjunction with laser-induced grating measurements, but typically involve the interference between a signal beam and an externally supplied reference beam.<sup>9</sup> In our technique, the reference is the internally

(36) Polonski, T.; Dauter, Z. *J. Chem. Soc., Perkin Trans. 1* **1986**, 10, 1781–1788.

(37) Charney, E.; Tsai, L. *J. Am. Chem. Soc.* **1971**, 93, 7123–7132.

(38) Luk, C. K.; Richardson, R. S. *J. Am. Chem. Soc.* **1974**, 96, 2006–2009.

(39) Lewis, J. W.; Goldbeck, R. A.; Kligler, D. S.; Xie, X.; Dunn, R. C.; Simon, J. D. *J. Phys. Chem.* **1992**, 96, 5243–5254.

(40) Kligler, D. S.; Lewis, J. W. *Rev. Chem. Intermed.* **1987**, 8, 367–398.

(41) Goldbeck, R. A.; Kligler, D. S. *Spectroscopy* **1992**, 7, 17–29.

(42) Xie, X.; Simon, J. D. *Rev. Sci. Instrum.* **1989**, 60, 2614–2627.

(43) Bjorling, S. C.; Goldbeck, R. A.; Milder, S. J.; Randall, C. E.; Lewis, J. W.; Kligler, D. S. *J. Phys. Chem.* **1991**, 95, 4685–4694.

generated signal from the intensity grating. If two linearly polarized laser beams, whose polarizations are neither parallel nor perpendicular, are crossed to form a grating in a chiral sample, both an intensity and a polarization grating will be formed. However, these two gratings will be spatially out-of-phase by  $\pi/2$  and will not interfere with one another. The diffracted probe light will then be proportional to the sum of the squares of the two grating amplitudes. When the polarization of one of the pump beams to prepare elliptically polarized light is controlled, both the amplitudes and the phases of the intensity and polarization gratings can be controlled to produce an interference (or heterodyne) between them. When the polarization is modulated to alternate between constructive and destructive interference of the gratings, one can essentially use the fairly small polarization grating to create large changes in the intensity grating and the overall signal.

In the experiments described here, the polarization of the pump beams was controlled by rotating a polarizing prism before the PEM. Because the rotation was over very small angles, the intensity of the incident beam was essentially unchanged. While there are other methods for altering the pump beam polarization, this scheme is the easiest to analyze theoretically. In this scheme, only two gratings are formed in the sample—one polarization grating and one intensity grating—and the phase can be controlled by the PEM retardation to produce completely constructive and destructive interference. Therefore, a plot of  $\Delta S/S_{\text{ave}}$  vs angle of rotation (as shown in Figure 7) reveals the dissymmetry ratio directly ( $\Delta\epsilon/\epsilon \approx \theta_{\text{peak}}$  for small values of  $\theta_{\text{peak}}$  measured in radians). However, if the experiment requires significant rotation of the polarizing prism, difficulties can be encountered. Some of the simplifying theoretical assumptions regarding small angles may break down, and experimentally, misalignment of the laser beams can occur due to walking of the beam through the polarizer.

We have investigated some other schemes for varying the incident polarization which have given consistent results with the experiments presented here and which may be more appropriate in specific experimental situations. For example, rotation of the PEM, rather than the polarizing prism, also produces the heterodyne CD signal and appears less likely to cause beam walkoff. An accurate theoretical treatment of this experiment involves four gratings—two polarization and two intensity—and does not produce complete cancellation of the signal. The theoretical limiting value of  $\Delta S/S_{\text{ave}}$  is therefore less than 2. While the value of  $\Delta\epsilon/\epsilon$  cannot be determined as directly in such an experiment, the theoretical treatment presented in this paper is applicable and the experimental data can be modeled quite well to determine the dissymmetry ratio. While the acceptance angle of a PEM is much greater than that of other polarization modulating devices such as a Pockel cell, multiple reflections within the PEM can cause additional complications when using a PEM with a coherent laser source. Proper alignment of the PEM is therefore fairly critical and rotation of the PEM can cause additional challenges.

We have also been successful at measuring CD by varying the PEM retardation for a fixed, nonzero angle of rotation of either the polarizing prism or the PEM, and by combining both rotation and PEM retardation. Measuring the signal as a function of the PEM retardation is perhaps the simplest laboratory procedure employed since the very small rotations (much less than  $1^\circ$ ) of optical elements shown in our results is unnecessary. However, these measurements require an accurate calibration of the PEM retardation over a large range of settings. A very promising compromise appears to be rotating the angle of either the polarizer or the PEM while using a reduced (less than quarter wave) retardation setting on the PEM. The PEM

only needs to be calibrated at this single setting, and while the limiting value of  $\Delta S/S_{\text{ave}}$  is still below 2, the peak of the  $\Delta S/S_{\text{ave}}$  curve (as shown in Figure 7) is shifted to larger angles and larger, more reasonable, steps in the rotation angle can be used to map out the response of the sample.

## Conclusions

The techniques described here represent a significant advance in making measurements of circular dichroism and appear to provide a basis for continued progress into more specialized experiments. The large  $\Delta S/S_{\text{ave}}$  signals, produced by very small values of  $\Delta\epsilon/\epsilon$ , are orders of magnitude larger than those found in conventional CD measurements. The increased sensitivity created by these high contrast measurements should provide a faster and more direct technique for detecting chemicals with small dissymmetry ratios. Since the input laser beams can be tightly focused and cross over such a short distance, the technique allows the use of short path length sample cells and ultrasmall probe volumes and offers a convenient and effective interface to analytical separation systems (e.g., liquid chromatography or capillary electrophoresis).

In addition, the ability to make measurements with pulsed laser systems allows for the extension of the technique to time-resolved measurements of CD. Because different regions of the CD spectrum can reveal specific information on the configuration and structure of a molecular system, a tunable method of measuring real-time changes in circular dichroism is of great importance for monitoring dynamics such as protein folding and rearrangement. In contrast to some other techniques for measuring time-dependent CD based on the oscillation frequency of a polarization modulator, the time scale and resolution of the experiment using the transient grating method described here is only limited by the absorption process and therefore by the pulse length of the laser system employed. Although artifacts such as linear dichroism induced by an initiating laser may create additional thermal gratings in such experiments, the phase of these gratings can also be determined and the heterodyne method may provide a convenient way to either avoid or directly measure such effects.

While the new CD measurement technique described here shows great promise, there are still experimental features to be enhanced and improved. As with all CD techniques, artifacts due to polarization optics and sample cells, must be overcome. While synchronization of a 50 Hz laser with a 50 kHz PEM works well here, the use of higher repetition rate lasers would further improve the duty cycle of the experiment. Phase-sensitive detection with lock-in amplifiers may also help for higher repetition rate experiments with lower overall signal levels or more stray light. Finally, combining the heterodyne techniques with phase-matched detection of thick gratings may improve the sensitivity significantly and allow for the extension of CD measurements to smaller values of  $\Delta\epsilon/\epsilon$  and to gas phase samples.

**Acknowledgment.** We gratefully acknowledge partial support of this work from Sandia National Laboratories Office of Laboratory Directed Research and Development. J.A.N. thanks the United States Department of Energy for an AWU-DOE Graduate Fellowship, and W.G.T. acknowledges partial support from the National Institute of General Medical Sciences, the National Institutes of Health under Grant No. 5-R01-GM41032. The authors thank Andre Epink for help with setting up the delay scheme for the polarization modulation and Mark Jaska for technical support in the laboratory.